Numerical Investigation of Turbulent Combustion Noise Using a Hybrid LES/CAA Approach

S. Herff, K. Pausch, M. Meinke, W. Schröder

published in

NIC Symposium 2018
K. Binder, M. Müller, A. Trautmann (Editors)

Forschungszentrum Jülich GmbH,
John von Neumann Institute for Computing (NIC),
Schriften des Forschungszentrums Jülich, NIC Series, Vol. 49,
ISBN 978-3-95806-285-6, pp. 413.
http://hdl.handle.net/2128/17544

Numerical Investigation of Turbulent Combustion Noise Using a Hybrid LES/CAA Approach

Sohel Herff[1], Konrad Pausch[1], Matthias Meinke[1,2], and Wolfgang Schröder[1,2]

[1] Institute of Aerodynamics, RWTH Aachen University, 52062 Aachen, Germany
E-mail: {k.pausch, s.herff, m.meinke, office}@aia.rwth-aachen.de

[2] Jülich Aachen Research Alliance (JARA-HPC), RWTH Aachen University, 52062 Aachen, Germany

The acoustic response of round turbulent flames is investigated by a hybrid large-eddy simulation / computational aeroacoustics (LES/CAA) with respect to the burner geometry and inflow turbulence distribution. The first study is conducted to extend the findings for a rectangular slot burner studied by Schlimpert *et al.*[22] to round burners. The results show that the round flame is more stable than the rectangular slot flame due to the additional expansion direction and the initial curvature. Consequently, smaller flame front perturbations and less flame pockets are generated at the flame tip reducing the noise emission in this region. Compared to the round burner, the additional length scale of the rectangular slot burner leads to a medium frequency region in the heat release spectrum with a stronger roll-off behaviour and a lower peak frequency in the acoustic spectrum. In the second study, the hybrid approach is used to investigate the impact of the inflow turbulence on the flame's acoustic emission. It is evident that various turbulence distributions lead to different turbulent kinetic energy spectra in the low frequency region of the cold jet. These differences also result in changes of the flame motion and significantly influence the acoustic spectra in the low frequency regime. Furthermore, a non-reactive LES computation including the burner's plenum revealed significant differences in the turbulent kinetic energy spectrum compared to the LES results of the reduced domain.

1 Introduction

Research in combustion noise is increasingly gaining interest for mainly two reasons. First, it is expected to become an important contributor to the overall sound emission of future jet aero engines, since the sound emission of the other components, such as jet noise, fan noise, etc., is being reduced through recent technological progress[1]. Second, combustion noise can lead to thermoacoustic instabilities. Especially the lean-premixed regime, which is favourable for achieving a highly efficient thermodynamic process with low emissions, is prone to an unstable feedback loop between the flame's unsteady heat release and its resulting acoustic emission that can lead to hazardous loads within the combustion chamber[2]. A deeper understanding of the acoustic source mechanisms is necessary for the prediction and avoidance of thermoacoustic instabilities in future combustor systems at lean premixed conditions.

Previous work has focused on acoustically excited laminar flames[4,5], and turbulent flames, such as diffusion flames[6,7], rich-premixed flames[8], and lean-premixed rectangular slot flames[9,10]. As a result, it was possible to characterise the acoustic response of a flame with respect to the hydrodynamic and shear layer effect. At flame Strouhal numbers (based on the flame length and the slot exit bulk velocity) of $St < 20$, the flames acoustic response to heat release perturbations, expressed by the flame transfer function $F_{pq} = [p'/p_0]^2/[q'/q_0]^2(St)$, where q denotes the integrated total heat release, shows a trend of αSt^2. For flame Strouhal numbers $St > 20$, however, a plateau region described by βSt^0 occurs. This tendency is observed for different flame parameters. For a detailed analysis, also with respect to the gas expansion ratio, the reader is referred to Schlimpert *et al.*[9]. In this study, the analysis is extended from rectangular to round configurations. First, a round flame with the same flame parameters as the previously investigated rectangular slot flame is computed to investigate the influence of the geometry on the acoustic response of the flame. Furthermore, a flame based on an experimental setup by TU Berlin[12] is simulated and analysed with respect to different turbulent inflow distributions.

2 Numerical Method

A hybrid LES/CAA approach is used for the analysis. In the first step, the flow field including the combustion process is computed by a large-eddy simulation (LES). Based on the LES results, the acoustic source terms and the mean flow field are used for solving the acoustic perturbation equations (APE)[3] in the second step to determine the acoustic fluctuations in the far-field. The hybrid approach allows for a numerically appropriate treatment of both the turbulent combustion process and the acoustic radiation at lower computational costs compared to the direct determination of the acoustic far field by an LES.

For the Large-Eddy Simulations the coupled flow/level-set solver ZFS is used[13,14], which is developed at the Institute of Aerodynamics. The conservation equations of a viscous compressible fluid are solved using an unstructured Cartesian grid flow solver, which is based on a strictly conservative finite-volume methodology[14,16]. The convective terms are discretised by a second-order accurate modified low-dissipation AUSM scheme and the viscous terms are approximated by second-order accurate central differences. The time integration is done by a third-order total-variation diminishing (TVD) Runge-Kutta scheme. A conservative cut-cell technique is used to capture arbitrary embedded boundaries. The flame surface movement is determined by the G-equation which is solved on the level-set grid. The spatial discretisation of the G-equation is a 5th order accurate upstream central scheme. The coupling of the flow solver with the G-equation solver is based on a dual grid approach, which allows an efficient adaptation of the Level-Set grid independently to the flow grid[14]. Hereby the G-equation is only solved in a narrow band around the flame front which is adapted during the simulation and thereby reduces the computational costs[16]. The mesh cells for the flow field are coupled to the Level-Set grid over a common coarse base grid. For the parallelisation the coarse cells are sorted along the Hilbert curve, which is then split into equally long pieces such that subdomains of the same computational weight are obtained. This subdomain decompositioning leads to a small surface to volume ratio such that a high parallel efficiency on a large number of CPU cores is achieved[10]. The determination of the acoustic field is based on the acoustic perturbation equations (APE)[3] for reactive flows[6], extended to account for high temperature gradients[18]. The APE describe the propagation of the acoustic waves in arbitrary mean flows while taking into account convection and refraction effects. The numerical method that is used to solve the APE-equations is based on a dispersion-relation-preserving summation by parts (SBP-DRP) scheme of 6th order[19] and a Runge-Kutta method in a low-dissipation, low-dispersion formulation[20]. The computations on JUQUEEN have been performed on up to 16384 processors for the largest LES setup with $87 \cdot 10^6$ cells. The CAA computations

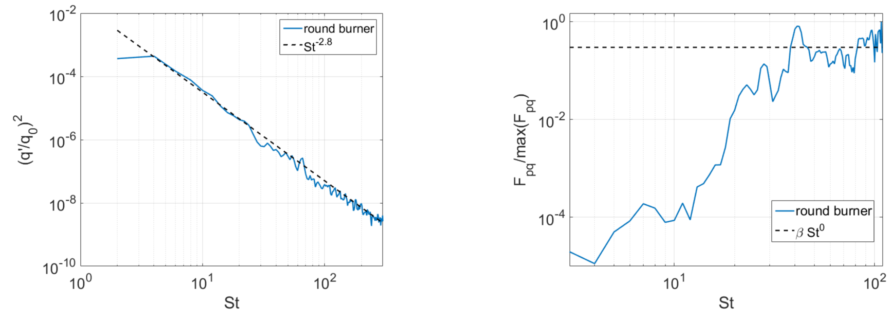

(a) (b)

Figure 1. Spatially integrated heat release (a) and acoustic response of the round flame (b).

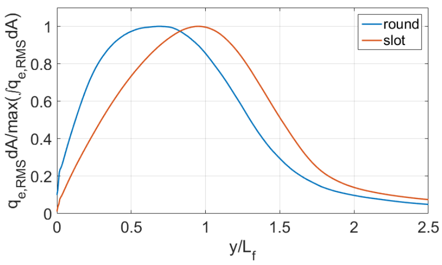

Figure 2. Indication of sound source location by horizontal integration of mean energy source fluctuations.

were conducted using 2048 cores in parallel. Multiple simulations incorporating different source terms were running at the same time.

3 Results

3.1 Impact of Burner Geometry

In this section, LES and CAA results of the round burner are analysed and compared with the results of the rectangular slot burner[9,10]. To investigate the geometry effect on the flame-acoustics interaction, the same parameters are used for the rectangular slot and the round flame. The Reynolds number $Re = 7000$ is based on the reference length D, where D is the diameter of the round burner, which is equal to the slot width D of the rectangular burner with a slot length of $L = 8.3D$. A lean-premixed methane-air mixture is burnt at an equivalence ratio of $\phi = 0.78$. For further details of the investigated configurations the reader is referred to Schlimpert *et al.*[9,26]. The near-field acoustic flame response to heat release fluctuations shown in Fig. 1 is similar to the findings of Schlimpert *et al.*[9]. That is, the acoustic spectrum is coupled to the heat release spectrum in the plateau region of the transfer function F_{pq} at $St > 40$.

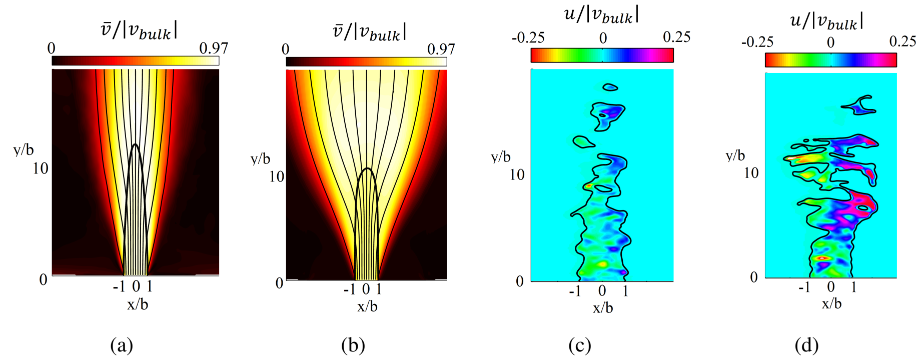

Figure 3. Mean axial velocity distribution (a, b) and instantaneous transverse velocity distribution (c, d) of the round (a, c) and the slot (b, d) burner.

However, differences are observed when analysing the source mechanisms. The horizontally integrated root-mean square (RMS) values of the fluctuations of the acoustic energy source are shown in Fig. 2. Similar to the findings of Rajaram and Lieuwen[23] for both flames, the maximum value, which is presumably connected to the axial location of maximum sound emission, is located near their mean flame length L_f. For the round flame, however, the maximum is located slightly further upstream of the mean flame length $y_{RMS_{max},round} \approx 0.75L_{f,round}$, whereas for the rectangular slot flame it is located at $y_{RMS_{max},rect.} \approx 0.95L_{f,rect.}$. This shows that compared to the round flame the rectangular slot flame generates more sound at its tip. The additional azimuthal expansion direction leads to a smaller streamtube widening and less streamline deflection, which reduces the hydrodynamic instability effect. Thus, smaller transversal velocity fluctuations are generated in comparison to the rectangular burner as shown in Fig. 3. Consequently, the more unstable rectangular flame shows enhanced flame surface perturbations, flame pocket generation, and annihilation. All of these mechanisms strongly contribute to the overall sound emission of the burner. For the round burner, however, the sound emission is less dominated by the flame instability. Hence, the turbulence of the shear layer exciting the flame surface near its base is expected to play a more important role for the round flame and is investigated in the following section.

3.2 Impact of Inflow Turbulence

For the numerical investigation of the impact of turbulence on combustion noise two computational domains are used. The first computational domain consists of $87 \cdot 10^6$ cells with local grid refinement leading to an isotropic cell spacing of $\Delta_{cell} = 0.0187D$ in the burner plenum and the jet region. The plenum, a turbulence grid which is positioned $3D$ above the bottom of the plenum, and the six annular injection drillings are included in this domain. The second computational domain is a subset of the first domain. It does not contain the plenum such that the inflow boundary is located just upstream of the converging nozzle. The mesh consists of $47 \cdot 10^6$ cells with the same cell spacing as the first domain. Synthetic turbulence is generated on the inflow boundary of the domain using the formulation of Batten *et al.*[24].

In the following the most important results are discussed. For further details to this study the reader is referred to Ref. 25. First, cold jets are considered. On the smaller domain, two inflow turbulence distributions are used. In the first case, denoted reduced domain computation 1 (RD1), the velocity distribution matches the experimental PIV measurements of the mean flow field at the nozzle exit, and the second case, denoted reduced domain computation 2 (RD2), approximates the turbulent kinetic energy spectrum on the inflow boundary region determined in the full plenum computation (FPC). Finally, the impact of the inflow turbulence distributions on the noise emission of the flame is analysed for the reduced domain computations and compared with the experimental measurements.

In Fig. 4 the mean flow statistics $0.4D$ downstream of the nozzle exit are shown. The black crosses are the measurement results. Strong fluctuations of the radial velocity component are observed at the centre of the cold jet. The mean statistics of the FPC are indicated by the black solid line. The mean results are in good agreement with the measurements and also the fluctuations of the radial velocity component are fully captured. The blue line in Fig. 4 shows the results for the RD1 case. The mean flow statistics are in good agreement with the experimental measurements with a slight underprediction of the radial RMS values.

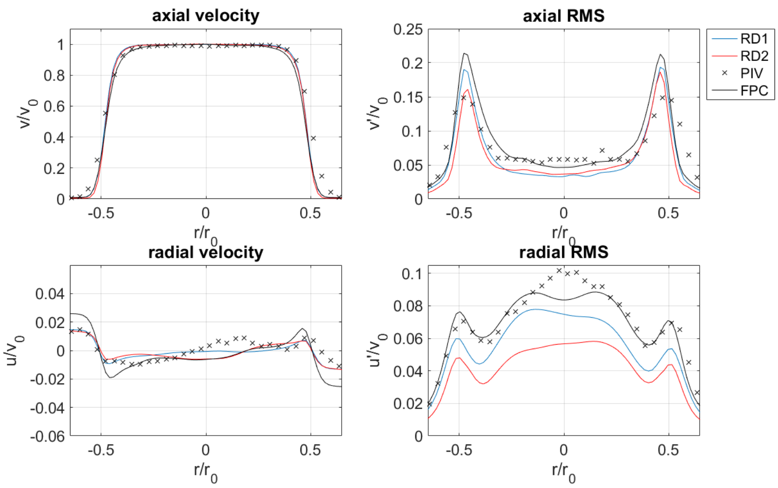

Figure 4. Mean and rms distributions of the axial and radial velocity components at $x/D = 0.4$ downstream of the burner exit. Black crosses are experimental measurements, the black line shows the full domain computation, the blue and red lines belong to RD1 and RD2.

The red line in Fig. 4 indicates the results of the RD2 case. Although the prescribed velocity fluctuations and the turbulent length scales differ from the RD1 case, the mean flow field of the RD2 case is similar to the RD1 case with slightly lower radial fluctuations. For details of the turbulent kinetic energy (TKE) spectra of these cases the reader is referred to Ref. 25. The flow in the RD1 and RD2 cases contains less turbulent kinetic energy than in the FPC case and will therefore lead to an underprediction of the flame movement for the combustion cases, which will be discussed in the next section.

In the following, the RD1 and RD2 cases are considered including the combustion process. These cases will be denoted CRD1 and CRD2. The mean heat release fields in Fig. 5 evidence differences in the mean flame shapes for the two cases. That is, the flame bases are similar but the flame length and flame tip shape differ. The differences in the flame dynamics lead to the acoustic spectra shown in Fig. 6b. The distributions of the sound pressure level (SPL) of the CRD1 and CRD2 cases and the spectrum of the spatially integrated heat release, illustrated in Fig. 6a, follow the same trend in the mid and high frequency range which is consistent with the findings of Rajaram and Lieuwen[23]. However, in the low frequency region the SPL of the CRD2 case is up to $10dB$ higher than that of the CRD1 case which is consistent with the higher kinetic energy in the low frequency region of the cold jet flows but not with the similar heat release spectra of the CRD1 and CRD2 cases. Due to the lower turbulent kinetic energy level of the CRD1 and CRD2 cases compared to the FPC case the overall SPL from the CAA results is lower than that of the measured SPL. The spectral acoustic trend is in good agreement for both computations.

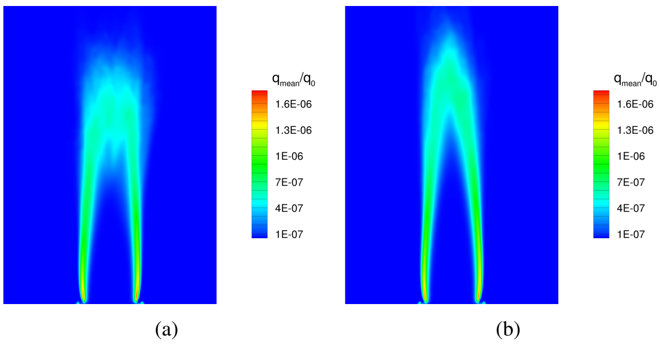

Figure 5. Mean heat release q_{mean} of CRD1 (a) and CRD2 (b).

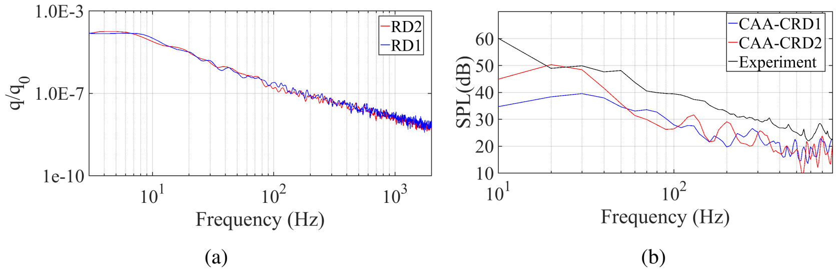

Figure 6. PSD of the spatially integrated heat release of CRD1 (blue) and CRD2 (red) (a) and PSD of the pressure signal (b). The black solid line indicates the measurements, the blue and red lines belong to RD1 and RD2.

4 Conclusions

The noise emission of turbulent flames has been numerically investigated using a hybrid LES/CAA approach. A comparison between a slot and a round burner reveals that the acoustic flame response to heat release fluctuations F_{pq} is similar for both setups. However, the noise generation mechanisms differ. Due to the more unstable nature of the rectangular burner, an enhanced growth of surface perturbations leads to more noise being generated near the flame tip indicated by the mean amplitude distribution of the energy source. Additionally, the impact of the inflow turbulence has been investigated for a round burner. Two synthetic turbulent inflow distributions have been used and the resulting flow field in the flame region was compared to experimental data. A computation of an extended domain, which includes the plenum and the radial injection of the experimental setup, revealed that the turbulent kinetic energy in the flame region is underpredicted by the LES for the reduced domain. Consequently, the acoustic emission of the reduced domain computations is lower compared to the experiment. It was shown that despite the differences between the two reduced domain computations in the inflow region, the mean flow fields and the turbulent kinetic energy spectra approach each other near the nozzle exit. However, the seemingly small differences between the cold jets already have an effect on the combustion noise in the low frequency region of the acoustic spectra causing differences in the sound pressure level of up to $10dB$. This illustrates the high sensitivity of combustion noise to the turbulent flow details. Therefore, a numerical investigation of the flame which includes the burner plenum will be performed in an upcoming study to capture and investigate all relevant details of the experiment.

Acknowledgements

This study was supported by the DFG Combustion Noise grant SCHR 309/43. The authors gratefully acknowledge the Gauss Centre for Supercomputing e.V. (`www.gauss-centre.eu`) for funding this project by providing computing time through PRACE on the GCS Supercomputer JUQUEEN at Jülich Supercomputing Centre (JSC).

References

1. A. Dowling and Y. Mahmoudi, *Combustion Noise*, P. Combust. Int. **35**, 65–100, 2015.
2. T. Lieuwen and V. Yang, *Combustion Instabilities in Gas Turbine Engines: Operational Experience, Fundamental Mechanisms*, AIAA J., 210, 2015.
3. R. Ewert and W. Schröder, *Acoustic perturbation equations based on flow decomposition via source filtering*, J. Comput. Phys. **188**, 365–398, 2003.
4. S. Schlimpert, S. Hemchandra, M. Meinke, and W. Schröder, *Hydrodynamic instability and shear layer effect on the response of an acoustically excited laminar premixed flame*, Combust. Flame **162**, 345–367, 2015.
5. S. Schlimpert, M. Meinke, and W. Schröder, *Nonlinear analysis of an acoustically excited laminar premixed flame*, Combust. Flame **163**, 337–357, 2016.
6. T. Bui, W. Schröder, and M. Meinke, *Acoustic Perturbation Equations for Reacting Flows to Compute Combustion Noise*, Int. J. Aeroacoustics, 335–355, 2007.

7. T. Bui, W. Schröder, and M. Meinke, *Numerical analysis of the acoustic field of reacting flows via acoustic perturbation equations*, Comp. Fluids, 1157–1169, 2008.
8. G. Geiser, A. Hosseinzadeh, H. Nawroth, F. Zhang, H. Bockhorn, P. Habisreuther, J. Janicka, C. O. Paschereit, and W. Schröder, *Thermoacoustics of a turbulent premixed flame*, AIAA Paper, 2014–2476, 2014.
9. S. Schlimpert, S. Koh, K. Pausch, M. Meinke, and W. Schröder, *Analysis of combustion noise of a turbulent premixed slot jet flame*, Combust. Flame **175**, 292–306, 2017.
10. K. Pausch, S. Schlimpert, S. Koh, J. Grimmen, and W. Schröder, *The Effect of Flame Thickening on the Acoustic Emission in Turbulent Combustion*, AIAA Paper, 2016–2745, 2016.
11. I. Duran, S. Moreau, F. Nicoud, T. Livebardon, E. Bouty, and T. Poinsot, *Combustion Noise in Modern Aero Engines*, Journal Aerospace Lab, 7, 2014.
12. H. Nawroth and C. Paschereit, *High-Speed Flow Field Measurements of Turbulent Jet Flames Undergoing Shear Layer Manipulation*, AIAA Paper, 2016–1841, 2016.
13. C. Günther, M. Meinke, and W. Schröder, *A flexible multiple level-set method for capturing and tracking moving embedded interfaces*, Comput. Fluids **102**, 182–202, 2014.
14. D. Hartmann, M. Meinke, and W. Schröder, *A level-set based adaptive-grid method for premixed combustion*, Combust. Flame **158**, 1318–1339, 2011.
15. D. Hartmann, M. Meinke, and W. Schröder, *A strictly conservative Cartesian cut-cell method for compressible viscous flows on adaptive grids*, Comp. Meth. Appl. Mech. Eng. **200**, 1038–1052, 2011.
16. D. Hartmann, M. Meinke, and W. Schröder, *Differential equation based constrained reinitialization for level set methods*, J. Comput. Phys. **227**, 6821–6845, 2008.
17. D. Hartmann, M. Meinke, and W. Schröder, *The constrained reinitialization equation for level set methods*, J Comput. Phys. **229**, 1514–1535, 2010.
18. S. R. Koh, G. Geiser, and W. Schröder, *Reformulation of Acoustic Entropy Source Terms*, AIAA Paper, 2011–2927, 2011.
19. C. K. W. Tam and J. C. Webb, *Dispersion-relation-preserving finite difference schemes for computational acoustics*, J. Comput. Phys., 107, 1993.
20. F. Hu, M. Hussaini, and J. Manthey, *Low-dissipation and low-disperion Runge-Kutta schemes for computational acoustics*, J. Comp. Phys. **124**, 177–197, 1996.
21. S. Schlimpert, M. Meinke, and W. Schröder, *Nonlinear analysis of an acoustically excited laminar premixed flame*, Combust. Flame **163**, 337–357, 2016.
22. S. Schlimpert, A. Feldhusen, J. H. Grimmen, B. Roidl, M. Meinke, and W. Schröder, *Hydrodynamic instability and shear layer effects in turbulent premixed combustion*, Phys. Fluids, 28, 2016.
23. R. Rajaram and T. Lieuwen, *Acoustic radiation from turbulent premixed flames*, J. Fluid Mech. **637**, 357–385, 2009.
24. P. Batten, U. Goldberg, and S. Chakravarthy, *Interfacing statistical turbulence closures with large-eddy simulation*, AIAA J. **42**, 485–492, 2004.
25. S. Herff, K. Pausch, H. Nawroth, S. Schlimpert, C. O. Paschereit, and W. Schröder, *Impact of turbulent inflow distributions on combustion noise of lean-premixed flames*, AIAA Paper, 2017–3219, 2017.
26. K. Pausch, S. Herff, S. Schlimpert, M. Meinke, and W. Schröder, *Acoustic flame response of a round and a slot burner*, AIAA Paper, 2017–3360, 2017.